Wu and Brenner Supplementary Figure S1

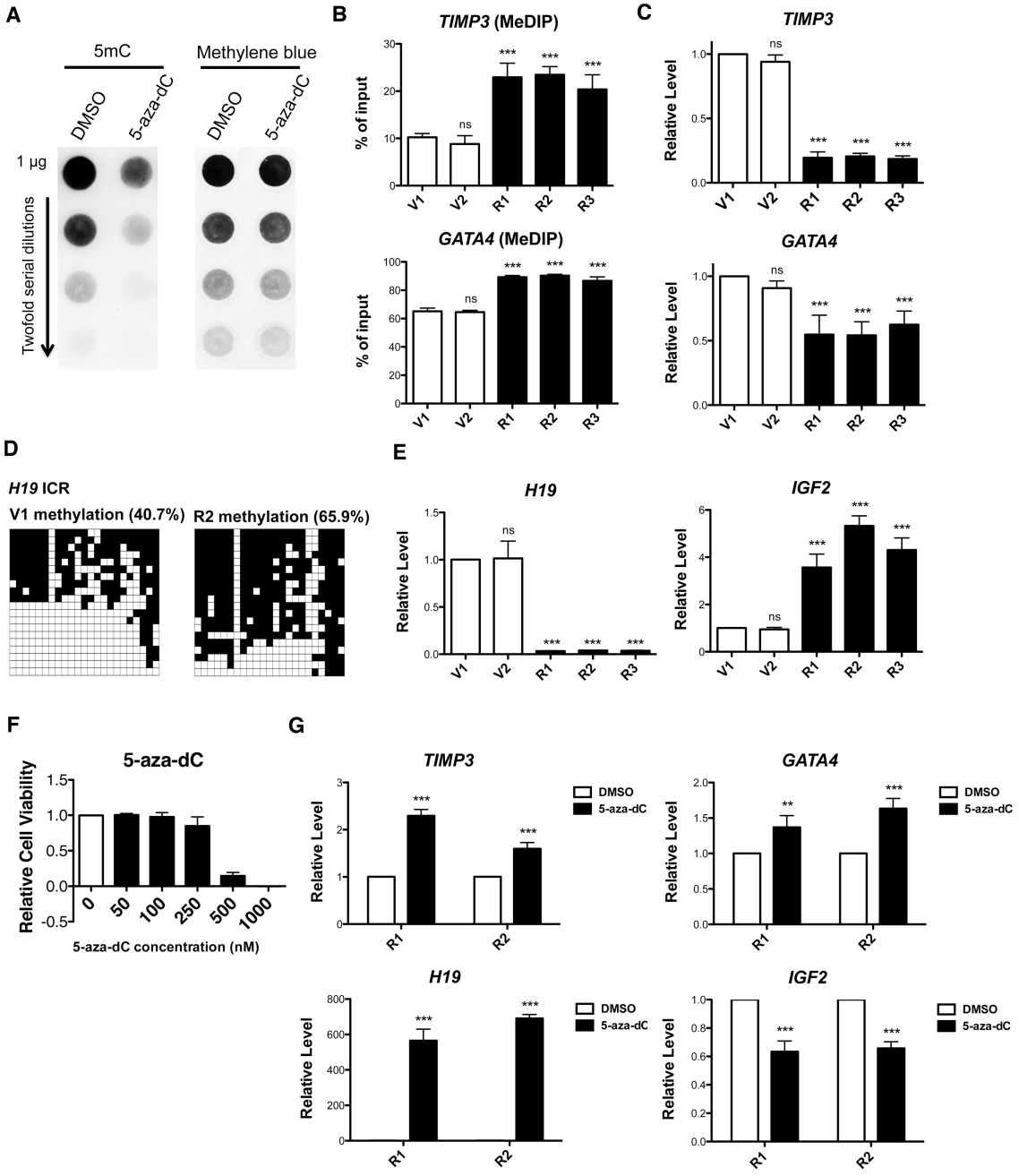

Figure S1. Oncogenic KRAS Expression Causes Hypermethylation-Mediated Silencing of TSGs and Loss of Imprinting, Related to Figure 2

(A) Genomic 5mC levels in HBEC3-R2 cells treated with DMSO or 5-aza-dC were measured by DNA dot blot.

(B) Methylation levels of promoter-associated CpG islands were analyzed by qPCR.
(C) mRNA levels were analyzed by RT-qPCR and normalized to V1 cells.
(D) 5mC bisulfite sequencing of *H19* ICR. White squares represent non-methylated cytosines and black squares represent methylated cytosines in CpG sites. The percentages of methylated CpG from 20 independent clones are indicated.
(E) mRNA levels were analyzed by RT-qPCR and normalized to V1 cells.
(F) HBEC3-R2 cells were treated with increasing concentrations of 5-aza-dC for 5 days. Cell viability was determined by resazurin and normalized to the DMSO treated control.
(G) After 5-aza-dC treatment, mRNA levels were analyzed by RT-qPCR and normalized to the DMSO treated control. All data are presented as mean ± SD. ns, no significant difference; **, $p < 0.01$; ***, $p < 0.001$ in comparison to V1 cells or the DMSO treated control.

Wu and Brenner Supplementary Figure S2

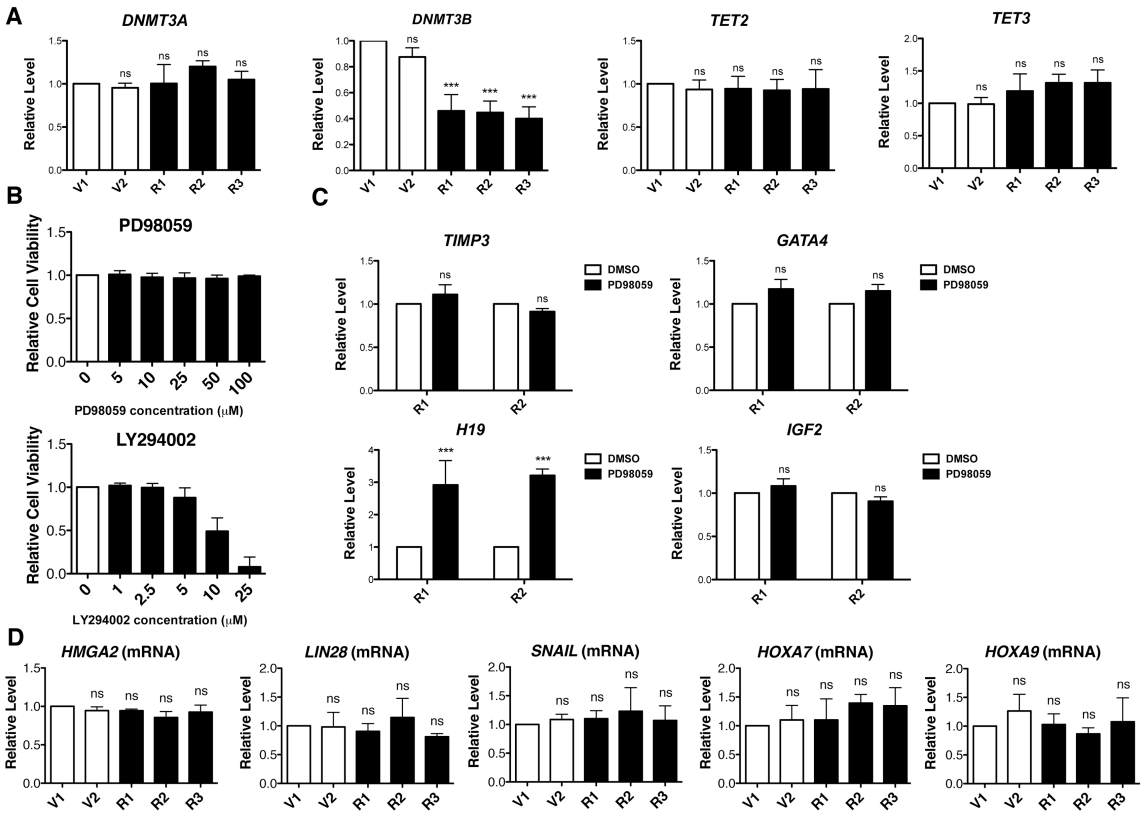

Figure S2. ERK Pathway Inhibition Reactivates Silenced *H19* Expression in KRAS cells, Related to Figure 3

(A) mRNA levels were determined by RT-qPCR and normalized to V1 cells.

(B) HBEC3-R2 cells were treated with increasing concentrations of PD98059 or LY294002 for 6 days. Cell viability was determined by resazurin and normalized to the DMSO treated control.

(C) After ERK pathway inhibition, mRNA levels were analyzed by RT-qPCR and normalized to the DMSO control.

(D) mRNA levels were determined by RT-qPCR and normalized to V1 cells.

Wu and Brenner Supplementary Figure S3

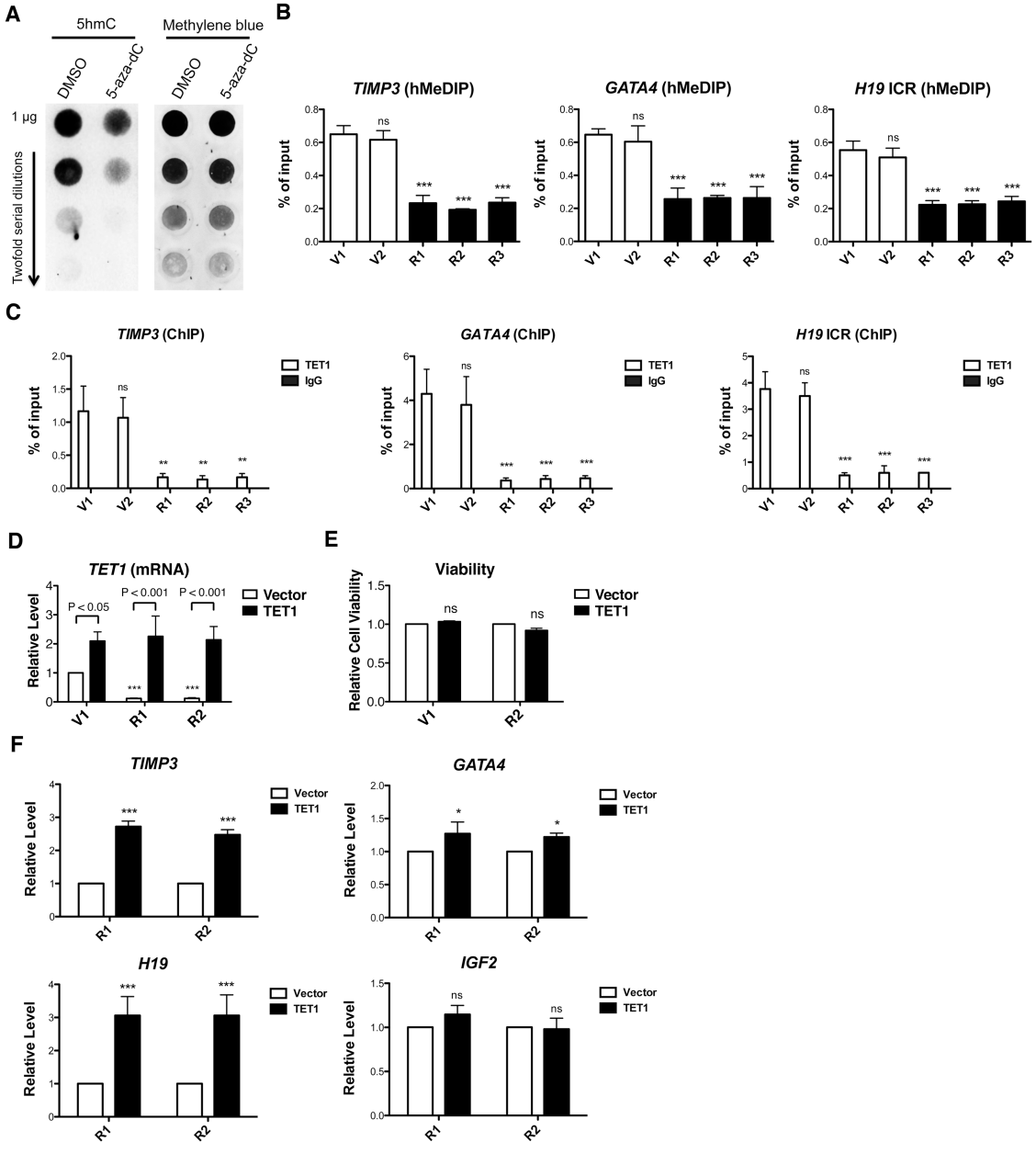

Figure S3. Reduction of 5hmC and TET1-Association are Responsible for KRAS-Mediated DNA Hypermethylation, Related to Figure 4

(A) Genomic 5hmC levels in HBEC3-R2 cells treated with DMSO or 5-aza-dC were measured by DNA dot blot.

(B) Hydroxymethylation levels of promoter-associated CpG islands were analyzed by qPCR.
(C) TET1 chromatin occupancy was analyzed using TET1 ChIP and qPCR.
(D) After TET1 viral transduction for 6 days, mRNA levels were analyzed by RT-qPCR and normalized to V1 cells with vector viral transduction.
(E) After TET1 viral transduction, cell viability was determined by resazurin and normalized to vector viral transduction.
(F) After TET1 viral transduction, mRNA levels were analyzed by RT-qPCR and normalized to the vector viral transduction control. All data are presented as mean ± SD. ns, no significant difference; *, $p < 0.05$; **, $p < 0.01$; ***, $p < 0.001$ in comparison to V1 cells or the vector virus control.

Wu and Brenner Supplementary Figure S4

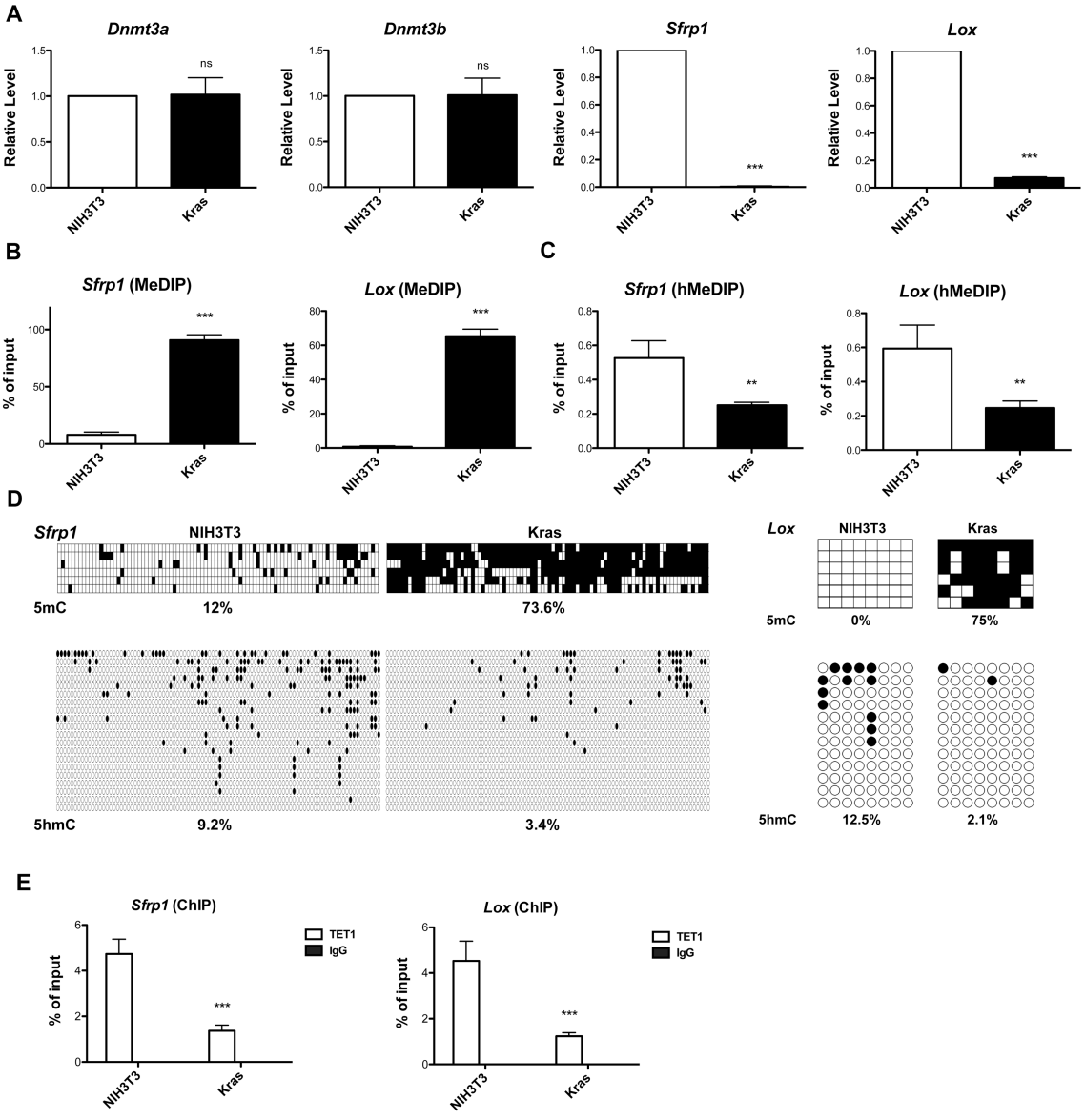

Figure S4. Kras-Mediated Suppression of Tet1 is Associated with Decreased 5hmC and Increased 5mC Levels, Related to Figure 5

(A) mRNA levels were determined by RT-qPCR and normalized to NIH3T3 cells. (B) Methylation and (C) Hydroxymethylation levels of *Sfrp1* and *Lox* promoters were analyzed by qPCR.

(D) Bisulfite sequencing for 5mC and TAB-seq for 5hmC. The percentages of 5mC or 5hmC are indicated at each promoter without and with Kras transformation.
(E) Tet1 chromatin occupancy was analyzed using Tet1 ChIP and qPCR. All data are presented as mean ± SD. ns, no significant difference; **, $p < 0.01$; ***, $p < 0.001$ in comparison to NIH3T3 cells.

Wu and Brenner Supplementary Figure S5

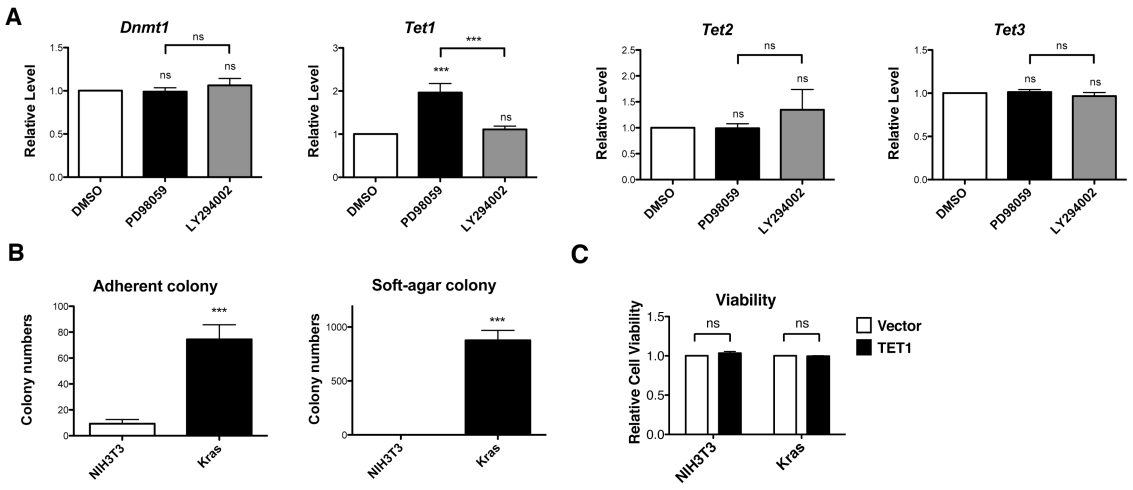

Figure S5. Erk Pathway Inhibition Increases *Tet1* Expression in Kras-Transformed NIH3T3 Cells, while Akt Pathway Inhibition Shows no Effect, Related to Figure 6

(A) After Erk pathway or Akt pathway inhibition, mRNA levels were analyzed by RT-qPCR and normalized to the DMSO control.

(B) Adherent and soft-agar colony formation.

(C) After TET1 viral transduction, cell viability was determined by resazurin and normalized to vector viral transduction. All data were presented as mean ± SD. ns, no significant difference; ***, $p < 0.001$ in comparison to the DMSO treated control or NIH3T3 cells.

Wu and Brenner Supplementary Figure S6

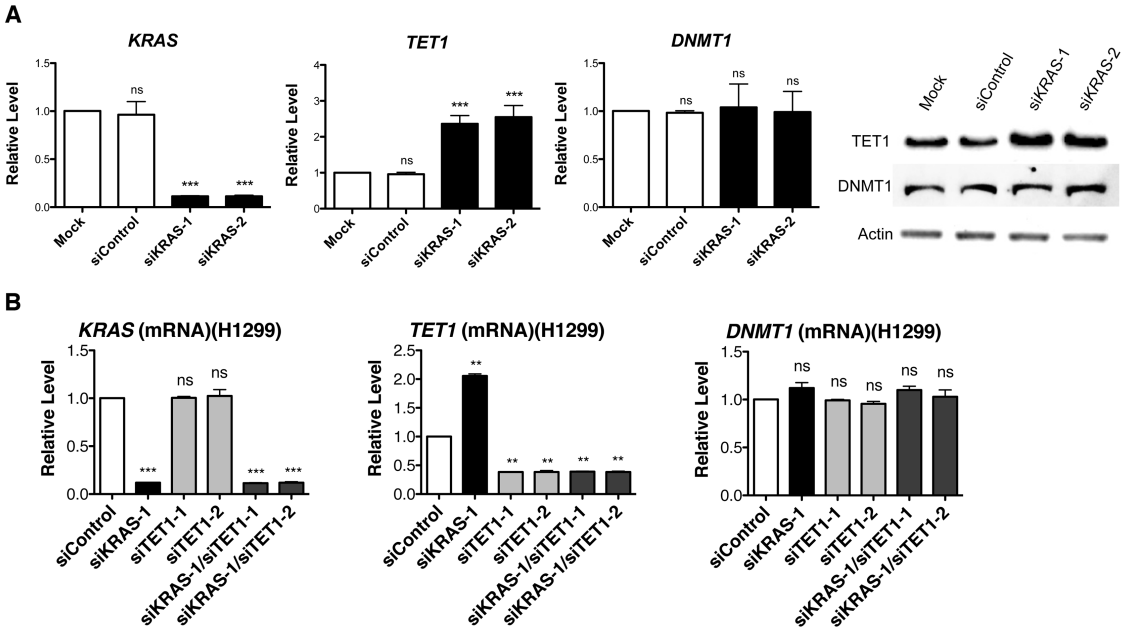

Figure S6. KRAS-Mediated Suppression of TET1 is Found in HepG2 Hepatoma Cancer Cells, Related to Figure 7

(A) After *KRAS* siRNA treatment, mRNA levels were determined by RT-qPCR and normalized to mock cells. Protein levels of TET1 and DNMT1 were determined by western blotting.

(B) After siRNA treatment, mRNA levels of H1299 cells were determined by RT-qPCR and normalized to siControl treated cells. All data are presented as mean ± SD. ns, no significant difference; **, $p < 0.01$; ***, $p < 0.001$ in comparison to mock cells or siControl treated cells.

Table S1. Target list of hypermethylated and silenced lung cancer TSGs, related to experimental procedures.

Function	Gene	Function	Gene
Cell Cycle	*P16*	**Cell Adhesion**	*CDH1*
			CDH13
Growth/ Differentiation	*APC*		*TIMP3*
	RARß		*TSLC1*
	DUOX1		*LAMA3*
	DUOX2		*RECK*
	IGFBP3		
	GATA4	**Apoptosis**	*DAPK*
	WWOX		*RASSF1A*
	MTHFR		*FHIT*
			FAS
DNA repair	*MGMT*		*NORE1A*
			BCL2
Detoxification	*GSTP1*		*SEMA3B*

Table S2. Human primers, related to experimental procedures.

	Forward	Reverse
Plasmid Construct		
***KRAS* TA Cloning**	CACCATGGAACAAAAACTTATTTCTGAAGA AGATCTGACTGAATATAAACTTGTGG	GTCGACTTACATAATTACACACTTTG
***TET1* TA Cloning**	CACCATGGAACAAAAACTTATTTCTGAAGA AGATCTGGAACTGCCCACCTGCAGCTG	GTCGACTCAGACCCAATGGTTATAGG
mRNA		
GAPDH	GAGTCAACGGATTTGGTCGT	GACAAGCTTCCCGTTCTCAG
KRAS	TGTGGTAGTTGGAGCTGGTG	TGACCTGCTGTGTCGAGAAT
DAPK	CTCCCCATTTCTTGGAGACA	CCAGGGATGCTGCAAACTAT
MGMT	ACGCACCACACTGGACAGCC	CCGGCACGGGGAACTCTTCG
DUOX1	ATGTGCCAGATACCCAAAGC	CAGCTGACGGATGACTTGAA
TIMP3	CTGACAGGTCGCGTCTATGA	AGTCACAAAGCAAGGCAGGT
GATA4	CCGGGATCTGCCGCGTTCTC	GGAGTGAGGGGTCTGGGCGT
H19	CCTCCACGGAGTCGGCACAC	GGCGCTGCTGTTCCGATGGT
IGF2	CGAATTGGCTGAGAAACAATTGGC	TCGGATGGCCAGTTTACCCTGAAA
DNMT1	GAGCTACCACGCAGACATCA	CGAGGAAGTAGAAGCGGTTG
DNMT3A	CAAGCGGGACGAGTGGCTGG	TCAGTGGGCTGCTGCACAGC
DNMT3B	CTCAGAGGCAGTGACAGCAG	TGTCTGAATTCCCGTTCTCC
TET1	ACCCCCTGTCACCTGCTGAGG	GCGATGGCCACCCCACCAAT
TET2	TCACACCAGGTGCACTTCTC	GGATGGTTGTGTTTGTGCTG
TET3	TCTCCCCAGTCTTACCTCCG	CCAGGCTTCAGGGAACTCAG
HMGA2	ACCCAGGGGAAGACCCAAA	CCTCTTGGCCGTTTTTCTCCA
LIN28	TGCGGGCATCTGTAAGTGG	GGAACCCTTCCATGTGCAG
SNAIL	TCGGAAGCCTAACTACAGCGA	AGATGAGCATTGGCAGCGAG
HOXA7	CCGCATTGAAATCGCCCAC	GGACCTTCGTCCTTATGCTCT
HOXA9	CTGTCCCACGCTTGACACTC	CTCCGCCGCTCTCATTCTC
MeDIP/ hMeDIP/ ChIP		
DAPK	GCTTTTGCTTTCCCAGCCAGGGC	ATCGCACTTCTCCCCGAAGCCAA
MGMT	GAACGCTTTGCGTCCCGACG	CCGAGGGAGAGCTCCGCACT
DUOX1	CCATGGGACTTGTGAAGGCGGAC	CTCCCGGGGCGCAGGTAGAG
TIMP3	GGGCCGATGAGGTAATGCGGC	GCCTGGGCGGCCGAGTGATA
GATA4	TGCTGGGGGAGCTTTCCGCACA	TGACTGGCCTGTGGGAGTCACGTG
***H19* ICR**	CTCACACATCACAGCCCGAG	TGTGGATAATGCCCGACCTG
Bisulfite sequencing		

***DAPK* 1st PCR**	TTTTATTTATTTTTTAGTTGTGTTTT	TAAAAACAATCTCTCTCCAACCTAC
***DAPK* 2nd PCR**	TTAGTTTTTGTTTTTTTAGTTAGGG	AACAATCCCCAAAACCACAT
***MGMT* 1st PCR**	GTTTTTTTGTTTTTTTTAGGTTTT	CAACATAAAAAAATAAAAAAAACCC
***MGMT* 2nd PCR**	GTTTTTTTGTTTTTTTTAGGTTTT	CCAATCCACAATCACTACAAC
***DUOX1* 1st PCR**	GGTTTTGGATTTGGAGTTTAGATT	AAAAAACTAACATTCCCCTTTCTTC
***DUOX1* 2nd PCR**	GTTTTATGGGATTTGTGAAGG	CTACCCTTAAAACTCCCTCCC
***H19* ICR 1st PCR**	TAGGGTTTTTGGTAGGTATAGAGTT	AAATCCCAAACCATAACACTAAAAC
***H19* ICR 2nd PCR**	ATATGGGTATTTTTGGAGGTTTTTT	AAATCCCAAACCATAACACTAAAAC

Table S3. Mouse primers, related to experimental procedures.

	Forward	Reverse
mRNA		
β-Actin	AGAGGGAAATCGTGCGTGAC	CAATAGTGATGACCTGGCCGT
***Dnmt1* (*)**	GAACCATCACCGTGCGAGAC	CCAGTGGGCTCATGTCCTTG
Dnmt3A	TGGTGCTTTCAAAACAGCGAG	GTTTGTTAAAACCCCCTCCAGC
Dnmt3b	ACTTGGTGATTGGTGGAAGC	CCAGAAGAATGGACGGTTGT
Tet1	TGTCAGACATGGGGCATCAG	TGTCGGGGTTTTGTCTTCCG
Tet2	TTGTTAGAAAGGAGACCCGGC	TCATGTCCTGTTGACCGTGAG
Tet3	CCGGCCGAGGTGGAAATAAATG	CCCTGAGGTGCTTAGCTGC
***Fas* (*)**	GATGCACACTCTGCGATGAAG	CAGTGTTCACAGCCAGGAGAAT
***Sfrp1* (*)**	CATCCATGGGGCTACAGTGA	TGGCATGGTGAGTTTTCAGG
***Lox* (*)**	CTCATCTGCCTGAAAGCACAC	GGGCAAAGAGGTACATCGAAG
MeDIP/ hMeDIP/ ChIP		
***Fas* (*)**	GAAGTAGAAACAGAAGCTGAG	TTGCTACATCCCAACTGTAAC
Sfrp1	TTACAGCGTCCAACTCCGAC	CGGCCAGAAGGATCGGTTTA
***Lox* (*)**	GCTGCTAGGACCTTGTGATGG	CACCCCAGATGAGAGGCCCA
Bisulfite sequencing		
***Fas* PCR (*)**	GAAAAGAAGTAGAAATAGAAGTTGAG	CTACATCCCAACTATAACTTTACTAC
***Sfrp1* 1st PCR (*)**	GAAAGTATTTGTTTAGTTTTTGGTTTTG	CAAATTAAACAACACCATTCTTATAACC
***Sfrp1* 2nd PCR (*)**	GTTTTGTTTTTTAAGGGGTGTTGAT	TTATAACACAACCTCAAATCCAC
***Lox* 1st PCR (*)**	AGGGAGGGGGTTGTTAGGATTTTG	TAACAACCACCCTCTCTCCTTTCACTC
***Lox* 2nd PCR (*)**	GTTGTTAGGATTTTGTGATGGTGAGTTG	CACCCCAAATAAAAAACCCATTCACTTAC

* Gazin, C., Wajapeyee, N., Gobeil, S., Virbasius, C.-M., and Green, M.R. (2007). An elaborate pathway required for Ras-mediated epigenetic silencing. Nature *449*, 1073–1077.

Supplemental Experimental Procedures

RT-qPCR

Total RNA was extracted using the RNeasy Mini Kit (Qiagen) with DNase treatment (Qiagen) to eliminate DNA contamination. Equal amounts of RNA were reverse transcribed to generate cDNA using an iScript cDNA Synthesis Kit (Bio-Rad). Specific primer pairs were then used to amplify target genes (Table S2 and S3). qPCR reactions were conducted with iQ SYBR Green Supermix (Bio-Rad). All data were collected from 3 or 4 independent experiments.

Immunoblotting

Protein extracts from each stable cell lines were prepared in RIPA buffer (Thermo Scientific) according to the manufacturer's instructions. Equal amounts of protein were separated using NuPAGE® Novex® 4-12% Bis-Tris Gel and transferred to 0.2 μm nitrocellulose membrane at 4 °C overnight. Proteins were detected using specific antibodies and visualized by SuperSignal West Femto Substrate (Thermo Scientific). Primary antibodies include TET1 (09-872, Millipore); DNMT1 (WH0001786M1, Sigma); RAS (05-1072, Millipore); myc Tag (05-724, Millipore); actin (ab3280, Abcam); Phospho-AKT (4060, Cell Signaling); Total-AKT (9272, Cell Signaling); Phospho-ERK (9101, Cell Signaling) and Total-ERK (9102, Cell Signaling). Secondary antibodies are goat anti-rabbit IgG (Thermo Scientific) and goat anti-mouse IgG (Thermo Scientific).

Proliferation Assay

1,000 cells were seeded in replicates of 6 in KSFM media with or without EGF supplementation in 96-well plates. Relative cell numbers were analyzed using resazurin (Sigma) 72 hrs after seeding. All data were collected from 4 independent experiments.

Adherent and Soft-agar Colony Formation

For adherent colony formation, 50 (HBEC3) or 200 (NIH3T3 and H1299) cells were seeded on 6-well plates, allowed to grow for 9 (NIH3T3), 10 (H1299) or 12 (HBEC3) days, followed by 4% methylene blue (Sigma) staining. Colony size > 2 mm were counted. For soft-agar colony formation, 10,000 cells were resuspended in media with 0.4% agarose and plated over a layer of 0.6% agarose. Cells were incubated at 37 °C for 3 (NIH3T3 and H1299) or 4 (HBEC3) weeks and colonies were stained with MTT (Sigma). Colony images were acquired with ChemiDoc XRS (Bio-Rad) and quantified using Quantity One software (Bio-Rad). All data were collected from 2 or 3 independent experiments, each in triplicate.